Double phase-retarder set-up at beamline P09 at PETRA III

2013 J. Phys.: Conf. Ser. 425 132010

(http://iopscience.iop.org/1742-6596/425/13/132010)

Journal of Physics: Conference Series **425** (2013) 132010 doi:10.1088/1742-6596/425/13/132010

Double phase-retarder set-up at beamline P09 at PETRA III

S Francoual[1], J Strempfer[1], D Reuther[1], D K Shukla[1] and A Skaugen[1]
[1] Deutsches Elektronen-Synchrotron DESY, Notkestr. 85, 22607 Hamburg, Germany

Abstract. Beamline P09 at PETRA III, DESY, is designed for general diffraction and resonant X-ray scattering experiments at low temperatures and high magnetic fields. The dependence of the X-ray cross-sections (Thomson, non-resonant magnetic, resonant exchange scattering, ATS) on the polarization state of the incident X-rays is an important property that one might want to capitalize on in a diffraction experiment. To that purpose, P09 is equipped with a double phase-retarder and diamond phase-plates making for the production of linearly and circularly polarized X-rays in the energy range between 3.5 and 8.5 keV as yet. Here we describe the double phase-retarder setup at P09, its principles of operation and its performances with respect to the generation of linearly polarized incident X-rays rotated by a variable angle η around the X-ray beam using two quarter-wave plates in series or a single half-wave plate.

1. Introduction

Different phase-plate configurations can be used to generate linearly polarized X-rays at arbitrary angles η around the X-ray beam. Although this is already possible with a single half-wave plate (1/2WP), two quarter-wave plates (1/4WP) in series may also be used for this purpose. Likewise two one-eighth wave plates (1/8WP) might be used to generate circularly polarized X-rays rather than one single 1/4WP. Though using two phase retarding plates is at the cost of intensity, there are offsetting advantages compared to just using a single plate. First, for experiments requiring alternating left and right circularly polarized light, using two 1/8WPs in series in a 90 degree geometry ensures that the X-ray beam sees the same effective thickness and that the transmitted intensity is the same for left and right circularly polarized X-rays [1]. Second, the deviation angle for 1/4WP (1/8WP) condition is 2 (4) times farther away from total Bragg diffraction than the deviation angle for 1/2WP condition; hence the amount of unpolarized X-rays, P_{un}, is reduced. Furthermore, the phase-shift changing more slowly as a function of the angular offset at 1/8WP (1/4WP) condition than at 1/4WP (1/2WP) condition, the phase-shift spread due to the divergence of the beam is reduced and depolarization effects are minimized. In case two 1/4WPs are used, it has been shown recently that the 90 and 180 degree geometries reduce the spread in phase shift due to the energy spread and to the divergence of the beam respectively as compared to the parallel geometry and yield higher degree of linear polarisation [2, 3].

2. Double phase-retarder at beamline P09 and diamond phase-retarding plates

The double phase-retarder (Huber Diffraktionstechnik GmbH & Co. KG) is shown in Figure 1. The phase-retarder consists of two Eulerian cradles, χ_1 and χ_2, separated by 340 mm. Each χ circle is equipped with two ϕ goniometers opposite to each other acting as θ and 2θ circles. The θ goniometers have positioning accuracy of 0.18″. They are equipped with a ± 10 mm Z (Z_S) translation making it possible to mount 3 phase-retarding plates at once and with a piezo-actuator aimed at the fast switching of the helicity of circularly polarized X-rays. The χ cradles are mounted on separate Z (Z_T) and X (X_T) stages to bring their centre of rotation on the beam axis. The rotation axes of the two χ

cradles are aligned parallel to each other better than 0.1°. A pitch and a yaw rotation below the bottom plate (not shown) further help aligning the whole assembly precisely along the beam axis. Rotating χ by 90°, the Bragg condition is kept within ±5″ in θ for the 2nd χ cradle with respect to the position χ_2= -45° and within ±10″ for the 1st χ cradle respect to the position χ_1=+45°. The double phase-retarder sits in its own UHV tank right after the monochromator and before the two mirrors [4]. This location implies that all its components are UHV compatible so as to maintain a vacuum better than 10^{-7} mbar. It also implies that the size, angular and energy spread of the beam incident on the plates are solely affected by which monochromator crystal pair is in use, the working energy and the amount of detuning of the second monochromator crystal with respect to the first. The divergence of the beam at P09 at the position of the phase-retarder is 9.4×6.5 μrad^2 at 6.5 keV (H×V) yielding a beam size of 1.18×0.85 mm^2 (FWHM). The energy resolution is $\Delta E/E = 1.3\times10^{-4}$ for Si(111). Effects of the detuning on the value of E and ΔE have been discussed elsewhere [5, 6]**.** For detuning less than 70% of the intensity of the fundamental, ΔE remains the same, if not smaller, hence the degree of linear polarisation, P_{LIN}, might not be altered. On the other hand, detuning deflects the beam requiring to realign the pitch and the height of the whole phase-retarder assembly.

Diamond is the best material for phase retardation at the energies between 3.5 keV and 15 keV due to its large structure factor, its low Z and its small mosaicity [7]. Six type-Ib diamond crystals are currently installed in the double phase-retarder at P09: two 400 μm (0,0,1) plates, two 200 μm (1,1,1) plates and two 100 μm (1,1,1) plates allowing for control of polarisation between 3.5 and 8.5 keV at transmission rates above 10 %. The crystals were oriented by back-scattering Laue diffraction and mounted so that the two (1,1,1) and (-1,-1,1) reflections lie in the ring plane when $\chi_1=\chi_2=0$. The plate holders were precision-machined within 0.5° to the shape of the plates in order to guarantee the orientation (see insert Figure 1). At present, we use the plates equally in asymmetric transmission-Laue and symmetric transmission-Bragg geometries although those are different cases within the dynamical theory of X-ray diffraction and different results might be expected with respect to the amount of circular polarisation in 1/4WP condition [8]. In Figure 2 we show the 1/4WP angular offsets

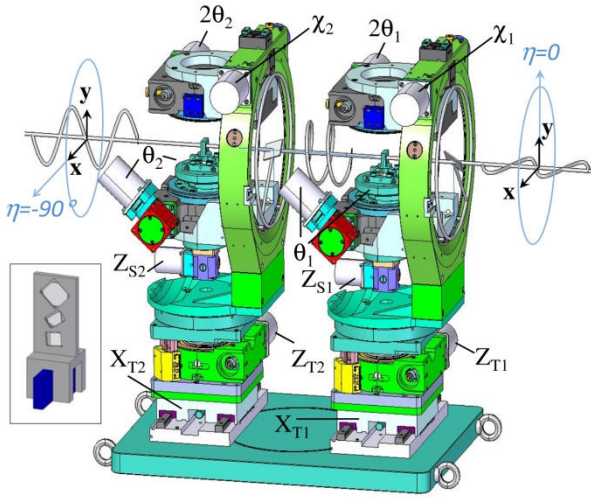

Figure 1. Double phase-retarder at P09 (see text). Superimposed thick grey lines: example of behavior of the polarization having a 1st 1/4WP at χ_1 = 45° and a 2nd 1/4WP at χ_2 = -45 in the 90 degree geometry. Insert: holder shaped to hold three diamond plates with sizes from 6×6 to 4×4 mm^2.

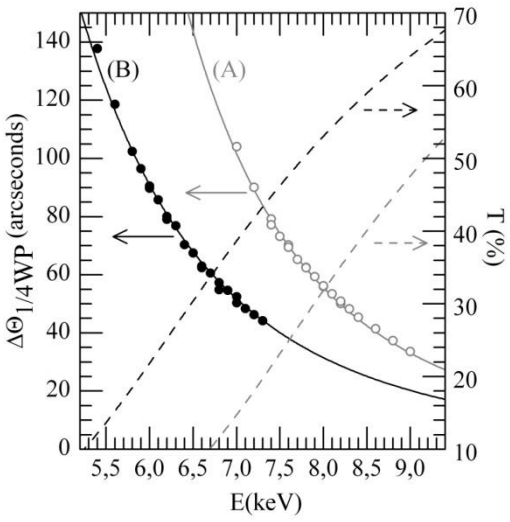

Figure 2. Measured angular offsets $\Delta\theta_{1/4WP}$ (circles; left axis) and calculated transmission rates (dashed lines; right axis) for the 400 μm (001) plates for the two glancing angles $\theta_{g,B}$ (black) and $\theta_{g,A}$ (light gray) *vs.* energy. Solid lines are a fit to $\Delta\theta_{1/4WP}$ using equation 1 in [7].

measured at several different energies for the 400 μm plates. Two glancing angles on the plates are considered to set the (1,1,1) and (-1,-1,1) in diffraction: $\theta_{g,A}= (54.73-\theta_{111})$ and $\theta_{g,B}=(54.73+\theta_{111})$.

3. Linear polarisation scans and performances of 400 μms (001) diamond plates

A major practical application of the double-phase retarder at P09 is for linear polarization scans *i.e.* for the generation of linearly polarized incident X-rays rotated by variable azimuthal angle η around the incident X-ray beam and analysis of the dependence upon η of the Stokes parameters P_1' and P_2' of the scattered signal from a sample. In table 1, we give the relation between η and the roll angles χ_1, χ_2 and phase shifts Φ_1, Φ_2 of the 1st and 2nd crystal plate. A full rotation of η from 0 to -180° is possible by varying χ_2 from 0 to -90° only using, either configuration (I) or configuration (IV), or using configurations (II) and (III) both together.

Table 1. Combinations of wave-plates for linear polarisation scans

1 × 1/2WP, χ_1 varies	$\Phi_1 = \pi$ (-π)	$\eta = 2\chi_1$	(I)
2 × 1/4WP$_s$, $\chi_1 = \pi/4$, χ_2 varies	$\Phi_1 = \Phi_2 = \pi/2$	$\eta = (\chi_2+\pi/4)$	(II)
	$\Phi_1 = -\Phi_2 = \pi/2$	$\eta = (\chi_2-\pi/4)$	(III)
2 × 1/4WP$_s$, χ_1 and χ_2 vary, $\chi_2 = \chi_1 - \pi/2$	$\Phi_1 = \Phi_2 = \pi/2$	No rotation	
	$\Phi_1 = -\Phi_2 = \pi/2$	$\eta = 2\chi_1 = 2\chi_2$	(IV)

In figure 3, we report results of measurement of P_{LIN} and δη at 7500 eV for the 400 μm plates at glancing angle $\theta_{g,A}$ for the four different combinations listed in Table 1, where δη is defined as the deviation of η from its expected value given column 3 of Table 1. The degree of linear polarisation $P_{LIN}=\sqrt{(P_1^2+P_2^2)}$ and the angle of linear polarisation $\eta=\text{atan}(P_2/P_1)/2$ have been evaluated by carrying out a polarisation analysis of the direct beam [9]. Combinations (I) and (IV) yield a same characteristic sine variation of P_{LIN} and δη of a periodicity of 90° as a function of χ_2. This is P_{LIN}~1 at χ_2=-90 and χ_2=0 and P_{LIN} minimum at χ_2 ~ -45° and $\delta\eta \neq \langle\delta\eta\rangle$ but for χ_2 = 0, -45 and -90°. Configurations (II) and (III) present sine variations with a periodicity of 180° which are less typical. The observed variations for the four different combinations are in general very similar to those that would be obtained would Φ_1 and Φ_2 depart from π or π/2 yielding a non-zero P_3. However, to account for P_{LIN}

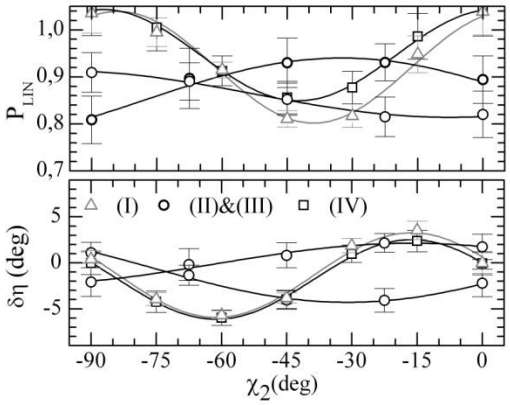

Figure 3. P_{LIN} and δη measured as a function of χ_2 at 7.5 keV for the different combinations of wave-plates listed in table 1 using the 400 μm plate at a glancing angle $\theta_{g,A}$. Lines are fits using a sine curve.

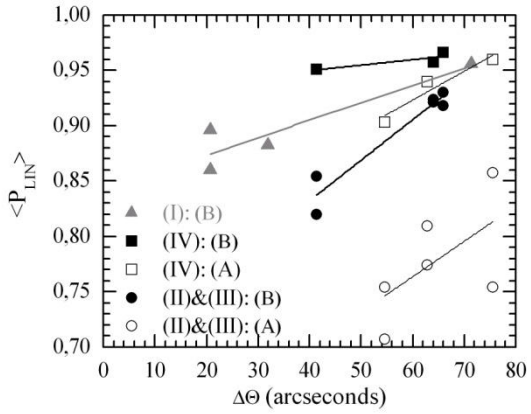

Figure 4. Mean value of P_{LIN} as a function of Δθ for the different combinations of wave-plates listed in Table 1 for the two glancing angles $\theta_{g,A}$ (A) and $\theta_{g,B}$ (B) and with χ_2 varying between 0 and -90°. Lines are linear fits.

and $\delta\eta$ in Figure 3 errors of 18″ on θ_1 and 3″ on θ_2 have to be considered which is rather unrealistic and points to additional reasons for the degradation of the linear polarisation. We note that in the case of an error of a few arcseconds on the positioning of θ_1 and θ_2 for 1/4WP or 1/2WP condition, combination (IV) always returns higher values of P_{LIN} than combinations (I),(II) or (III).

In Figure 4 we plot the mean value of $<P_{LIN}>$ measured as a function of $\Delta\theta$ for the 400 μm plates at glancing angles $\theta_{g,B}$ and $\theta_{g,A}$. Standard deviations are not shown for the purpose of clarity. For a same effective thickness and at the same deviation angle $\Delta\theta$, $<P_{LIN}>$ is higher when using two 1/4WPs in series in configuration (IV) *i.e.* the 90 degree geometry than in configuration (II) or (III). For all combinations, the lower the angular offset from the Bragg position, the lower the mean value of $<P_{LIN}>$. This trend results from multiple effects: (a) an error on the positioning of the plates of a few arcseconds < 5″ cannot be ruled out and would yield an admixture of circular and linear polarisation that has more consequences at low angular offsets and (b) the closer to total Bragg diffraction the higher the amount of unpolarized light. The mosaicity of the current 400 μm plates constrains $\Delta\theta$ to values larger than 40″. In the same line of idea it can be seen in Figure 4 that $<P_{LIN}>$ is considerably lowered by 5 to 10% when glancing angle is $\theta_{g,A}$: $\theta_{g,A}$ results in twice the total effective thickness compared to $\theta_{g,B}$. Type Ib diamond crystals have more defects than type IIa crystals. The beam incident onto the plates at the phase-retarder location at P09 is large and integrates over a large number of defects. The low glancing angles further increase this number resulting in lower $<P_{LIN}>$.

4. Conclusion

The double-phase retarder setup at P09 is operational and generates linear polarisation at arbitrary angles about the X-ray beam for the purpose of linear polarisation scans using different combinations of WPs. The higher degree of linear polarisation is achieved using two 1/4WPs in series in the 90 degree geometry. A single 1/2WP of half the total effective thickness also gives a reasonable amount of linear polarisation and might be advantageous to use at a same energy whenever intensity is an issue. It is important to be aware of the variations of P_1, P_2 and η as a function of χ_2 in Figure 3 when modelling P_1' and P_2' from a sample. In the near future the type Ib diamond plates will be replaced by type IIa plates for which a higher degree of linear polarisation is expected at the lower angular offsets [2,3]. Also an additional double phase-retarder will be available in the experimental hutch so that different types of WPs can be inserted and polarisation control at P09 is possible in a wider range of energy.

5. References

[1] Lang J. 2005 *APS Annual Report* 148-149
[2] Okitsu K, Ueji Y, Sato K and Amemiya Y 2001 *J. Synchrotron Rad.* **8** 33
[3] Scagnoli V, Mazzoli C, Detlefs C, Bernard P, Fondacaro A, Paolasini L, Fabrizi F and de Bergevin F 2009 *J. Synchrotron Rad.* **16** 778
[4] Strempfer J et al., *in preparation*
[5] Schulte-Shrepping H and Drube W 2001 *Nucl. Instrum. Methods Phys. Res.* A **467-468** 396-399
[6] Hou Z 2005 *Rev. Sci. Instrum.* **76** 013305
[7] Giles C, Malgrange C, Goulon J, de Bergevin F and Vettier C 1994 *Nucl. Instrum. Methods* **349** 622
[8] Hirano K, Ishikawa T and Kikuta S 1993 *Nucl. Instrum. Methods Phys. Res.* A **336** (1993) 343
[9] Detlefs C, Sanchez del Rio M and Mazzoli C 2012 *Eur. Phys. J. Special Topics* **208** 359

Acknowledgments

S. F. is grateful to C. Detlefs (ESRF) for introduction to the density matrix formalism for control of polarisation; J. S. acknowledges continued discussions with J. Lang (APS) and L. Bouchenoire (ESRF) about phase-retarder design and best material for phase-retardation; S. F. and J. S. thank V. Scagnoli (PSI) for discussing the performances of P09 phase-retarder.